Available online at www.sciencedirect.com
SCIENCE DIRECT®
Journal of African Earth Sciences 39 (2004) 133–145
Journal of African Earth Sciences
www.elsevier.com/locate/jafrearsci

Petrogenesis of the Kabanga–Musongati layered mafic–ultramafic intrusions in Burundi (Kibaran Belt): geochemical, Sr–Nd isotopic constraints and Cr–Ni behaviour

Jean-Clair Duchesne [a,*], Jean-Paul Liégeois [b], André Deblond [a,b], Luc Tack [b]

[a] Department of Geology, University of Liège, B20, B-4000 Sart Tilman, Belgium
[b] Royal Museum for Central Africa, B-3080 Tervuren, Belgium

Available online 16 September 2004

Abstract

A succession of mafic–ultramafic layered intrusions forms an alignment in the boundary zone between the Kibaran belt and the Tanzania craton. The intrusions represent a continuous series of cumulate rocks. For instance, in the Mukanda-Buhoro and Musongati (MBM) contiguous bodies, the series starts with dunite and passes to lherzolite, pyroxenite, norite, gabbronorite and anorthosite on top. Cumulate textures are conspicuous in all rock types and cryptic layering characterises cumulus mineral compositions, thus evidencing fractional crystallization as a major differentiation mechanism. The increase of Cr in the ultramafic members of the series indicates that chromite was not a liquidus mineral in dunite and lherzolite rocks, thus unable to form chromitite layers. The high Ni-content of dunite seems to preclude the existence of conjugate Ni-rich sulphide deposits. The $^{87}Sr/^{86}Sr$ initial ratio is relatively constant and averages 0.7087, with some values up to 0.712 due to local assimilation. Fine-grained rocks from the MBM area are isotopically (Nd and Sr) similar to the MBM cumulates. Modelling their crystallization produces cumulus mineral compositions similar to those in the Musongati ultramafic rocks, which suggests a broadly picritic parental magma. On the other hand, fine-grained rocks from the Nyabikere area are not related to the Nyabikere cumulates. Nd and Sr isotope ratios show that the MBM magmatism is related to an enriched source, possibly an old subcontinental lithospheric mantle. The Nyabikere dykes, as well as the Waga dykes, come from a depleted mantle source, as do the A-type granitoids occurring in the same boundary zone. Several lines of evidence point to two types of parental magmas, a picritic magma, and a more evolved magma, broadly similar to the Bushveld Main Zone magma.

Keywords: Burundi; Layered intrusions; Chromitite; Ni-sulphide; Chromite; Sr–Nd isotopes

1. Introduction

Layered gabbroic intrusions host the major Cr, Ni and PGE (platinum group elements) deposits (Naldrett et al., 1987; Cawthorn, 1996; Lee, 1996). It is now widely recognized (e.g. Evans, 1993) that the genesis of these orthomagmatic deposits is strongly controlled by the magma composition and magma chamber processes such as fractional crystallization (with or without contamination), immiscibility, and magma mixing. Petrological studies aiming at defining these processes are thus useful to evaluate mining potential and to plan exploration methods.

The purpose of the present paper is to investigate the petrology and geochemistry (major and trace elements, Sr and Nd isotopes) of a series of Kibaran layered intrusions in Burundi (Central Africa) in order to define magmatic processes, which have controlled their genesis, as well as the nature of their parental magmas. Geochemical characteristics of the rock series are also used to

* Corresponding author. Tel.: +32 43 66 22 55; fax: +32 43 66 2921.
E-mail address: jc.duchesne@ulg.ac.be (J.-C. Duchesne).

0899-5362/$ - see front matter © 2004 Elsevier Ltd. All rights reserved.
doi:10.1016/j.jafrearsci.2004.07.055

assess the metallogenic potential of the Burundian intrusions. This approach complements the general evaluation of mineral resources presented by Deblond and Tack (1999).

2. Regional geological setting

The Northeastern Kibaran Belt in Burundi (Fig. 1) comprises a Western Internal Domain (WID), made up of a deformed sequence of Mesoproterozoic granites and amphibolite-greenschist facies metasedimentary and metavolcanic rocks, overthrust on an Eastern External Domain (EED). The latter comprises supracrustal material, which is less deformed and metamorphosed and without granites, resting upon the Archaean Tanzania craton (Fig. 1; see references in Tack et al., 1994, 2002).

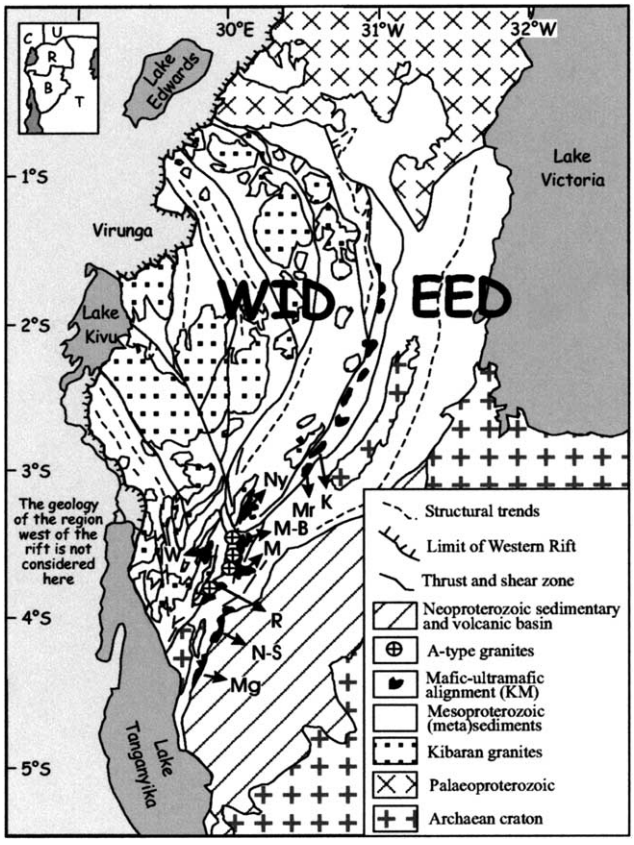

Fig. 1. Geological outline of the Northeastern Kibaran Belt, modified after Fig. 1 in Tack et al. (1994). The Archaean craton shown is a part of the Tanzanian craton; the Palaeoproterozoic is called the Buganda-Toro Belt in Uganda; the Kibaran granites are peraluminous (the representation includes pre-Kibaran Palaeoproterozoic relicts and post-Kibaran Sn-bearing granites); the Kabanga–Musongati (KM) mafic and ultramafic alignment and the A-type granitoids intrude the "Boundary Zone" between the Western Internal Domain (WID) and the Eastern External Domain (EED); the Neoproterozoic comprises the Bukoban–Malagarasian sedimentary and volcanic basin. K: Kabanga; M: Musongati; Mr: Muremera; Ny: Nyabikere; M-B: Mukanda-Buhoro; W: Waga; R: Rutovu; N-S: Nyange-Songa and Mg: Mugina. Inset: C = Congo; U = Uganda; R = Rwanda; B = Burundi; T = Tanzania.

A series of mafic and ultramafic intrusions straddles the border (Fig. 1: "Boundary Zone") between the WID and EED domains, together with some A-type granitoids (Tack et al., 1994). These intrusions form the Kabanga–Musongati (KM) alignment, named after the Kabanga intrusion in Tanzania, explored for Ni-sulphides (Evans et al., 1999, 2000), and the Musongati ultramafic intrusion in Burundi, a potential Ni lateritic deposit (Deblond and Tack, 1999 and references therein; Fig. 1). The emplacement age of the KM alignment is currently under debate. A previous 1275 Ma bulk zircon age (Tack et al., 1994) is challenged by a zircon SHRIMP set of measurements spreading from 1370 Ma to 1200 Ma; the 1370 Ma end-member is interpreted as the intrusion age (Wingate, zircon SHRIMP age in Tack et al., 2002). Preserved from pervasive deformation and metamorphism, the intrusions were only affected by brittle deformation associated with locally developed thrust faulting. A contact aureole of cordierite- and andalusite-bearing spotted metapelites, overprinting the regional schistosity, attests to their intrusive character at relatively low pressure and precludes an origin as part of a dismembered ophiolitic complex (Tack and Deblond, 1990).

Eight intrusions have been documented in Burundi (Deblond, 1993, 1994). They include (Fig. 1), from north to south, the Muremera, Nyabikere, Waga, Mukanda-Buhoro, Musongati, Rutovu, Nyange-Songa and Mugina intrusions. Among them, two broad types of intrusions can be defined: those which mainly consist of ultramafic rocks, such as Waga, Musongati, Nyabikere and Muremera, and those dominated by gabbroic rocks, such as Mukanda-Buhoro, Nyange-Songa, Rutovu and Mugina (Fig. 2, inset). In Tanzania, an updated distribution of the KM intrusions is given by Evans et al. (2000).

3. The Mukanda-Buhoro and Musongati intrusions

As an example, the Mukanda-Buhoro and Musongati contiguous bodies are focussed on because they associate all rock types and were extensively studied (Deblond, 1994; Fig. 2). At Buhoro, the mafic rocks occupy depressions in the landscape and are often ferralitised. Outcrops are scarce, but the rocks, frequently occurring as boulders, are surprisingly fresh. In the eastern part of Musongati, a thick laterite covers the ultramafic rocks and sampling is only possible through drilled cores. Both bodies have been sliced by imbricate thrust faults.

The Musongati body displays a series of thick layers, made up of different lithologies and dipping 60° on average to the west. The lower part of the structure consists of ultramafic rocks (dunite and lherzolite grading

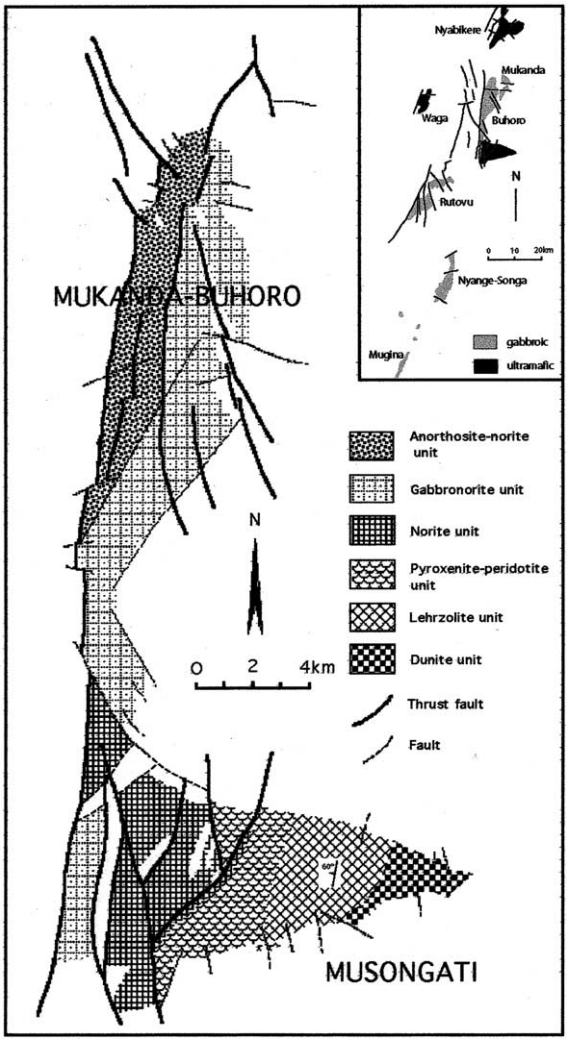

Fig. 2. Schematic geological map of the Mukanda-Buhoro and Musongati bodies. Inset: alignment of the two types of layered bodies in Burundi (the Muremera body, north of the area, is not shown).

upwards into alternating pyroxenites and peridotites), which pass into a mafic zone dominated by noritic rocks. Further to the west, a septum of metasediments clearly separates a norite unit belonging to the Musongati body from a gabbronoritic unit which is the southern extension of the Mukanda-Buhoro body (Fig. 2).

The rocks show typical characteristics of cumulates (Fig. 3). Olivine is euhedral in ultramafic rocks and the first liquidus mineral to appear in the sequence of rocks (Fig. 4). Fine-grained chromite is present in minor amounts in ultramafic rocks. In the dunite and lherzolite units, it occurs in the interstices between cumulus olivine, and never forms chromitite layers. This points to an intercumulus status. Plagioclase laths and prismatic orthopyroxene crystals define a conspicuous lamination in noritic and gabbroic rocks. In ultramafic rocks plagioclase shows an intercumulus habit. Sulphides (pyrrhotite, pentlandite, chalcopyrite) are disseminated in all

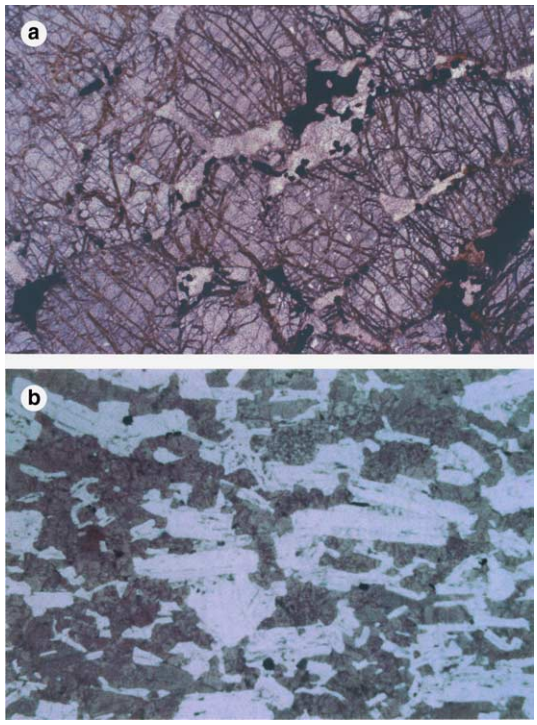

Fig. 3. Cumulate textures: (A) Peridotite (MU75) showing euhedral olivine (partly serpentinised); plagioclase, pyroxenes and opaques (chromite and sulphides) are intercumulus minerals; uncrossed nicols. (B) Gabbronorite (BU21) with clear igneous lamination, underlined by plagioclase laths; interstitial Ca-poor pyroxene (inverted pigeonite) forms large oikocrysts; uncrossed nicols. Lengths of the photos are 1.3 cm.

	Olivine Fo	Ca-poor px mg#	Ca-rich px mg#	Plag An	Fe-Ti oxides
anorthosite-norite unit		51-46 (6)	? 63-59 ?	66-57 (19)	
gabbronorite unit		58-45 (13)	67-57 (13)	75-58 (27)	
septum			septum		
norite unit		79-75 (4)	83-80 (4)	89-86 (20)	Chromite
pyroxenite-peridotite unit	88-83 (2)	80-85 (5)	83 (1)	88-80 (4)	? ?
lherzolite unit	88 (1)		90 (1)		
dunite unit	90-89 (3)		93 (1)		

Fig. 4. Stratigraphic succession of petrographic units and mineral chemistry variation (microprobe data of Deblond, 1994) in the Mukanda-Buhoro–Musongati layered intrusion. Cumulus minerals are represented by a continuous line, intercumulus minerals by a dashed line. Question marks indicate ambiguous cumulus/intercumulus status. Intercumulus Ca-poor pyroxene in the lherzolite and dunite units is usually altered. In brackets, number of determinations. Note that the Mwiriba quartz norite unit and the Mutanga amphibole norite unit, defined by Deblond (1994), are located in the upper part of the norite unit (Fig. 2) and have essentially the same cumulus mineral compositions.

rocks as minor components, but can locally attain a significant content in the dunite and lherzolite units. Fe–Ti

oxide minerals are present in the two upper units, and form a deposit in the Mukanda area.

It emerges from Figs. 2 and 4 that rocks more evolved than anorthosite are not known in the Mukanda-Buhoro intrusion. They might have been removed by erosion or faulting. The most evolved rock in all KM intrusions of Burundi has been found in the Mugina intrusion. It is an anorthosite (An_{56}) with fayalitic olivine (Fo_7) and inverted pigeonite (mg# 17) (Deblond, 1994).

It is noteworthy that gabbronorites in all considered KM intrusions are texturally similar to the Bushveld Main Zone cumulates, described by Wager and Brown (Fig. 213, p. 387 in Wager and Brown, 1968): slightly reversely zoned tabular plagioclases with local myrmekite define an igneous lamination. Inverted pigeonite also forms large poikiloblasts (up to 10 cm in diameter), as is also the case in the Bushveld Complex von Grünewaldt (1990).

Cryptic layering is conspicuous in cumulus mineral compositions (Fig. 4). Cumulus olivine varies from Fo_{90} to Fo_{76} and cumulus plagioclase from An_{90} to An_{76}. This evolution is parallel to the mg# variation of both pyroxenes. These characteristics strongly suggest that fractional crystallization was the major differentiation mechanism operating in the various magma chambers, as also noted by Evans et al. (1999) for the Kabanga intrusion.

4. Cumulate chemistry, the chromitite issue, and sulphide segregation

Whole rock chemical compositions of rocks coming from the Mukanda-Buhoro and Musongati (MBM) contiguous bodies, and from the other massifs, have been reported by Deblond (1994). Representative analyses of the main rock types are given in Table 1. Fig. 5 illustrates the evolution with all available data, for a few selected elements.

As expected the whole rock compositions are strongly controlled by the nature and proportion of the cumulus minerals. For instance, Al contents (Fig. 5) are very low in dunite. In lherzolite and pyroxenite it mainly represents the small amount of intercumulus plagioclase. In norite and gabbronorite, where plagioclase is a cumulus mineral, the Al_2O_3 contents range between 10% and 20% to reach a maximum of 27% in anorthosite.

The Cr-evolution is somewhat unexpected (Fig. 5) because Cr is typically a compatible element in basaltic magma, which usually sharply decreases in the successive liquids and cumulates of a fractional crystallization process. Here Cr tends to increase with declining MgO in the olivine-bearing ultramafic rocks. Cr concentrations culminate in the pyroxenite and rapidly decrease in norite to disappear in anorthosite. The most important Cr-carrier minerals in ultramafic rocks are chromite and pyroxenes. Deblond (1994) has shown that the Cr_2O_3 contents of Ca-rich and Ca-poor pyroxenes can be as high as 1.0% (sample RU12.53) and 0.73% (sample MU69), respectively. Considering Cr mineral/melt partition coefficient values of 34 for clinopyroxene and 10 for orthopyroxene (Rollinson, 1993), it can be inferred that the Cr melt composition was of the order of several hundred ppm when the pyroxenes appeared at the liquidus. These high values are reflected in the high Cr content of pyroxenite in Fig. 5. Actually, the behaviour of Cr in dunite and lherzolite shows a grossly defined increase, which is partly due to the increase with differentiation of the amount of Cr-rich pyroxene in the cumulate, and partly to the increase of the Cr content in the melt. Whatever the influence of the two factors, this behaviour certainly points to a melt not depleted in Cr. This in turn puts strong constraints on the value of the Cr bulk partition coefficient between dunite and lherzolite cumulates and melt. This must thus have evolved at values close to one, or even lower than one, which drastically limits the fraction of chromite in the cumulate. In other words, if chromite was an abundant liquidus mineral in the dunite and lherzolite cumulates, it would have determined a very high bulk partition coefficient for Cr and a rapid depletion of Cr in the successive melts. Chromite is indeed only found sporadically in dunite and lherzolite and always as a trace mineral. Though our data do not preclude occurrence of chromitite associated with pyroxenite, no chromitite layers analogous to those found in the Bushveld Complex or the Great Dyke have ever been observed. The present considerations suggest that there is a low probability to find chromitite deposits, thus limiting the Cr metallogenic potential of the studied layered bodies in Burundi.

The Ni-content shows an overall decrease with MgO (Fig. 5). Fig. 6 shows that there is no Ni–S correlation, thus indicating that the sulphides are not systematically Ni-rich. It also shows that Ni might be contained by pentlandite in some samples. Moreover, the high Ni values of two samples with very low S contents nevertheless indicate that, in these samples at least, olivine is Ni-rich. More data on olivine composition are obviously needed, but the present work suggests that the whole rock Ni-content might be controlled by olivine. The high Ni values observed in dunite (3000–4000 ppm) fall within the range commonly found in layered intrusions (see Simkin and Smith, 1970). This suggests that an immiscible Ni-rich sulphide melt did not segregate from the magma prior to its intrusion into the chamber. Such segregation would have depleted the coexisting silicate melt in chalcophile elements and PGE, and olivine would have been strongly depleted in Ni (Thompson and Naldrett, 1984; Naldrett, 1989). Therefore, unlike the occurrence of the Kabanga Ni-sulphide deposits in Tanzania (Evans et al., 1999, 2000), large bodies of massive Ni–Cu–Co sulphide

Table 1
Whole-rock major (%) and trace (ppm) element analyses of selected petrographic types from Kabanga–Musongati intrusions

	Dunite	Dunite	Peridotite	Peridotite	Pyroxenite	Pyroxenite	Norite	Norite	Norite	Gabbronorite	Gabbronorite	Anorthosite	Anorthosite
	F211.54*	F211.53*	MU74*	MU79A*	MU69	NY.P128	MU51	MU39	MU61	BU30	BU105**	MU31	BU85
SiO_2	38.34	37.69	44.10	43.12	53.19	51.33	52.57	49.28	49.18	50.89	49.65	47.56	51.98
$Ti0_2$	0.03	0.01	0.06	0.04	0.15	0.18	0.16	0.05	1.31	0.28	0.29	0.18	0.06
Al_2O_3	0.30	0.38	1.45	4.33	3.36	6.16	8.22	20.96	16.76	15.21	1549	2623	25.71
Fe_2O_3	13.44	13.15	14.24	15.37	11.86	13.59	13.52	6.82	13.66	13.34	12.65	5.91	3.33
MnO	0.16	0.17	0.21	0.17	0.18	0.20	0.23	0.10	0.24	0.20	0.19	0.10	0.04
MgO	47.30	47.74	38.88	32.43	28 05	24.27	20.32	10.27	5.60	7.49	7.03	3.86	0.99
CaO	0.22	0.10	0.04	3.96	2.36	4.88	5.45	11.74	10.62	10.86	11.87	14.55	13.21
Na_2O	0.10	0.01	0.07	0.01	001	0.25	0.37	0.85	1.46	2.08	1.97	1.33	3.49
K_2O	0.01	0.01	0.01	0.01	0.01	0.05	0.03	0.15	0.57	0.08	0.21	0.18	0.33
P_2O_5	0.01	0.01	0.01	0.01	0.01	0.01	0.02	0.04	0.05	0.01	0.02	0.02	0.01
Total	99.90	99.27	99.07	99.44	99.14	100.93	100.89	100.26	99.46	100.43	99.36	99.92	99.16
S (%)	1.23	0.0779	0.003	0.47	0.039	0.28	0.08	0.26	0.03	0.27		0.04	0.11
Zr	7	3	3	7	10	3	3	13	62	3	4.5	12	18
Hf				0.5	0.2	0.2	0.2	0.2	1.6	0.2	024	0.2	0.2
Nb	3	7	3	3	3	3	3	3	9	3	0.44	3	3
Ta				0.2	0.5	0.5	0.5	0.5	0.5	0.5	0.06	0.5	0.5
Rb	3	3	3	3	3	3	3	6	29	3	3.4	9	10
Sr	3	3	3	21	12	47	49	113	162	160	148	179	267
Ba	15	15	41	41	15	15	43	15	174	34	56	47	81
Ni	4048	2983	3377	1591	132	52	12	12	12	12	61	12	12
V	28	12	82	94	414	225	455	208	373	406	337	156	77
Cr	1704	2790	2746	3604	5027	3576	1710	1176	77	104	152	199	12
Zn	53	44	62	70	74	86	78	36	76	68	66	35	27
Co	155	164	150	143	100	92	40	12	37	65	43	12	12
La				0.2	1.0	0.9	1 1	3.1	13.1	1.3	1.9	3.2	3.3
Ce				4	4	5	1.5	6	27	15	3.0	6	7
Nd				2	02	2	2.5	2	12	2	2.2	2	2
Sm				0.1	0.2	0.2	0.2	0.5	2.5	0.5	0.79	0.4	0.6
Eu				0.1	0.2	0.2	0.5	0.7	1.0	0.5	0.67	1.0	0.8
Gd											1.02		
Tb				0.2	0.2	0.2	0.2	0.2	0.2	0.2	0.19	0.2	0.2
Yb				0.1	0.4	0.5	0.2	0.5	1.7	0.7	0.97	0.3	0.4
Lu				0.02	0.09	0.09	0.1	0.07	0.27	0.12	0.15	0.09	0.07
$[La/Yb]_n$				1.4	1.8	1.3	3.9	4.4	5.5	1.3	1.4	7.6	5.9
Eu/Eu*				0.8	1.3	1.3	3.2	3.0	1.4	2.2	2.2	4.9	3.1

Major elements by XRF analysis (CIGI, ULG) on calcinated samples; trace element at X-ray Assay Lab., Canada, except samples *by XRF and **by ICP MS (CIGI. ULG); S by XRF at X-ray Assay Lab., Canada.

Sample location: F211.54: Musongati body, bore hole 211, depth 54 m; F211.53: same, depth 53 m; MU74: Musongati body, Nyamabuye river;MU79A: Musongati body, Marumanga; MU69: Musongati body 1.5 km W of Nkeyuke; NY.P128: Nyabikere body, Ntaruka River, NE of Nyarurnazi; MU51:Musongati body, Miremera; MU39: Musongati body, Muhoza; MU61: Musongati body, Gihehe river 1km W of Miremera; BU30: Buhoro body, 500 m SW of Nyarurambi ; BU105: Buhoro body, Gihamagara Mu31: Musongati body; 500 m W of Nyarubimba; BU85: Buhoro body, Mutukura River, 1 km E of Shungwe.

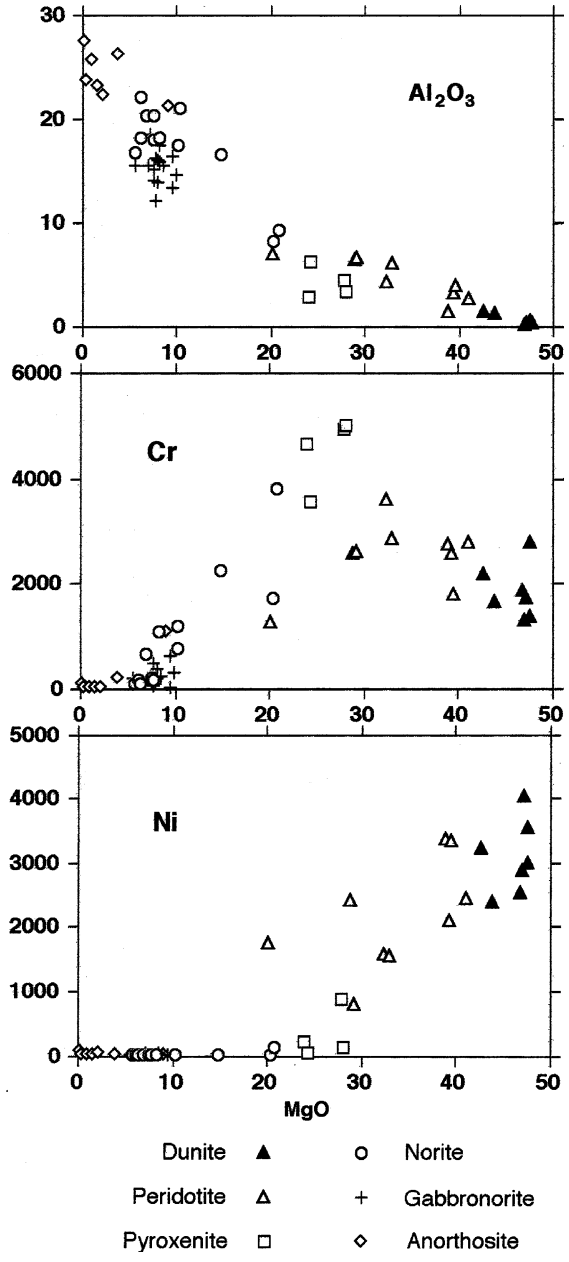

Fig. 5. Variation in whole-rock compositions: Al_2O_3 (%), Cr (ppm) and Ni (ppm) vs. MgO (%) (data from Deblond, 1994).

are not to be expected in the Musongati and Waga bodies in Burundi. On the other hand, S-saturation started during fractionation of dunite and gave rise to disseminated sulphides, which are depleted in Ni.

5. Strontium initial ratio in cumulate rocks

Sr isotopes have been studied in the various intrusions in order to identify different magma influxes (Kruger, 1994) and variations due to crustal assimilation. Detailed data are reported in and summarized in Fig. 7. The interval of variation of the Sr initial ratio, all massifs included, is relatively restricted: a first group contains 17 samples out of 21 and ranges from 0.7068 to 0.7089, and a second group of four samples ranges between 0.7104 and 0.7120 (Fig. 7). There is no definite relationship with the intrusion or with the rock type,

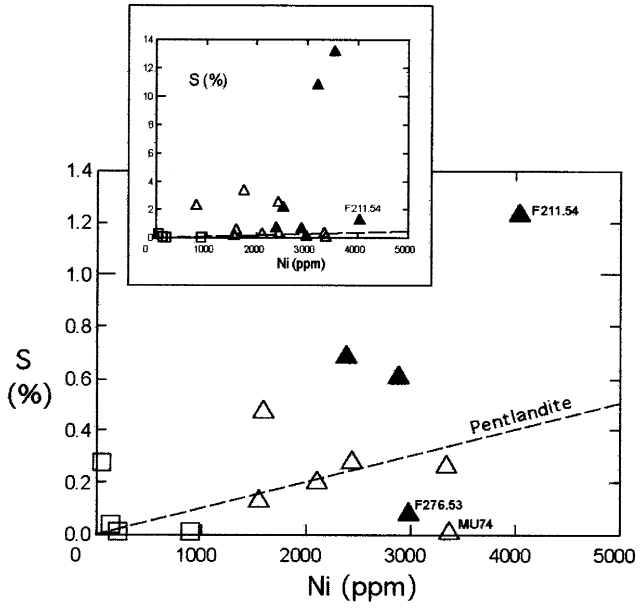

Fig. 6. S (%) vs. Ni (ppm) in ultramafic rocks (data from Deblond, 1994). Same symbols as in Fig. 5. The dashed line represents the Ni/S ratio in pentlandite $(Fe,S)_9S_8$ with Fe/Ni = 1, the richest Ni sulphide carrier in these rocks. Samples below this line have a Ni content not completely accounted for by pentlandite. Conversely, samples above the line contain sulphides other than pentlandite, i.e. pyrrhotite, pyrite and chalcopyrite. Samples on the line may contain pentlandite as the only Ni carrier. Note that six other samples with S > 1.4% (see inset) also fall in the S-rich field. Samples F276.53 and MU74 (Table 1) are very poor in S, thus Ni must be essentially contained in olivine.

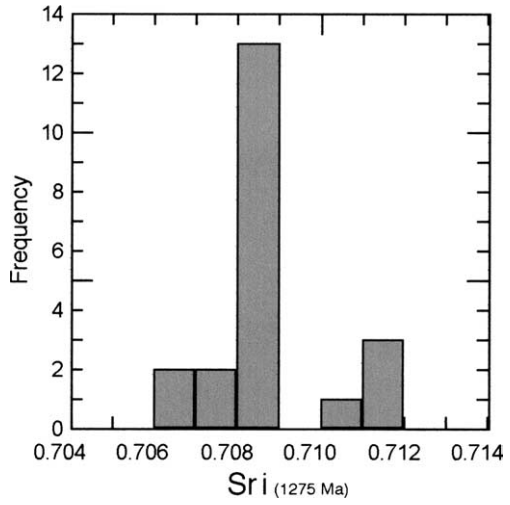

Fig. 7. Histogram of whole rock Sr isotope initial ratios at 1275 Ma (data from Deblond, 1993, 1994).

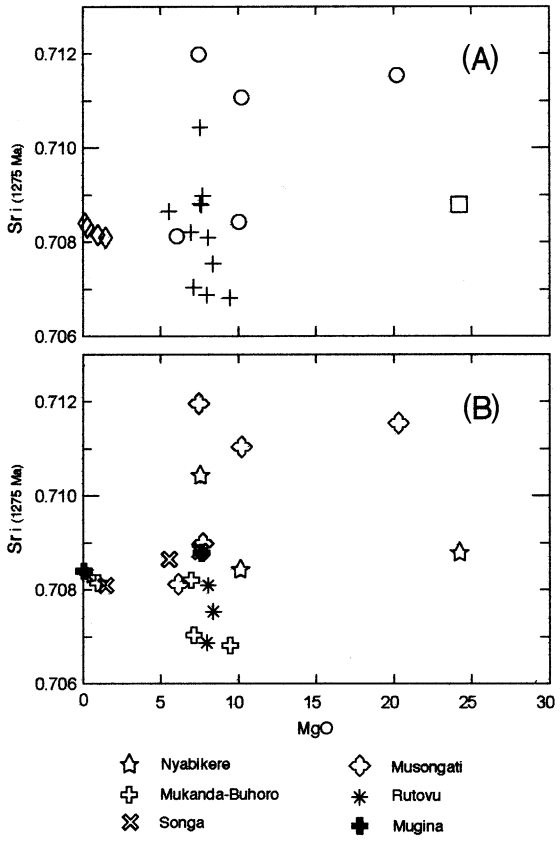

Fig. 8. Sr isotope initial ratio vs. MgO (%) whole-rock content. (A) Rock types, same symbols as in Fig. 5; (B) intrusions.

as illustrated in Fig. 8. The highest initial ratios are found in some noritic rocks, and the most evolved cumulates, i.e. anorthosites, are not different from the least evolved gabbronorite and pyroxenite. These characteristics suggest (1) that the high Sr initial ratios (second group) probably result from strong local contamination with country rocks, as also observed by Evans et al. (1999) in the Kabanga intrusion, and (2) that continuous assimilation during fractional crystallization (AFC process) was not significant. Variations within bodies are not related to structural height in the intrusion and distinct influxes of magma with different isotopic signature cannot be identified. The high average Sr initial ratio in group 1 thus appears to be related to the characteristics of the magma source rather than to an AFC process.

6. Geochemistry of related fine-grained rocks

No chilled margins have been identified in the various intrusions. The identification of possible melts, either parental or more evolved, has thus to rely on indirect evidence. Fine-grained rocks, with typical subophitic texture or with microgranular texture occur within the intrusions, preferentially close to the margins. In two cases, these fine-grained rocks belong to dykes cutting across the country rocks. Though the ages of these dykes are unknown, their occurrence at small distance from the main intrusions (Rutovu, RU04; S. Mukanda-Buhoro, 93BU4 and 93BU5) and their textural resemblance to the facies within the bodies strongly suggest that they belong to the same magmatic event. Classically such fine-grained rocks offer the best possible opportunity to define melts belonging to the same kindred as those forming the layered bodies. More evolved rocks, characterized by intersertal granophyric structure (A117B and NYP176; Table 2), have also been considered.

Major and trace element geochemistry as well as isotopes are used to check the cumulus vs. melt status of some of these rocks and the nature of the magma series to which they belong, in order to test possible contamination processes during differentiation, and to define the nature of the magma source. Data on major and trace elements are reported in Table 2 and isotopes in Table 3.

6.1. Major and trace elements

Out of the 16 cases considered (Table 2), the fine-grained microgabbros (SG23C, BU92, BU78 and RU10) cannot be considered as possible melts. They display a distinct positive Eu anomaly (Fig. 9) and low incompatible element contents. They show similarities with cumulate rocks and probably represent crystal–laden liquids. The two granophyric rocks (A117B and NYP176) are typically more differentiated with higher SiO_2, K_2O, Rb, Ba, HFSE and REE contents as well as negative Eu anomalies (Fig. 9 and Table 2). The rest of the samples can be divided into three groups, geographically and geochemically distinct. The first group comprises four fine-grained rocks related to the Mukanda-Buhoro body. This group is relatively enriched in silica (48–53% SiO_2) and LREE, and depleted in TiO_2, Sr and Nb (Fig. 10A and B). The mg# is close to 60. The second group is made up of fine-grained rocks from the Nyabikere area (Fig. 10C and D). Compared to the Mukanda-Buhoro group, the rocks are richer in Ti and Nb (no anomalies in spidergrams), the REE distribution has a constant slope, and the silica content (≈48%) and the mg# (≈50) are lower. The third group includes fine-grained rocks from Waga and Rutovu. The major elements are comparable to the Nyabikere group, but they show spidergrams depleted in incompatible elements and horizontal REE distributions (Fig. 10C and D).

6.2. Isotopes

Sr and Nd isotopic compositions have been measured on several melts. Table 3 shows the new data together with previously published data for some cumulate rocks

Table 2
Whole-rock major (%) and trace (ppm) element analyses of cumulate and finegrained rocks from Kabanga–Musongati intrusions

Type	SG23C	BU92	BU78	RU10	BU93	93BU4	93BU5	BU17	A117B	NY P176	NY P142	NY P145	NY P138	NY80	W26	RU04
	cum	cum	cum	cum	Buhoro	Buhoro	Buhoro	Buhoro	Rutovu	Nyabikere	Nyabikere	Nyabikere	Nyabikere	Nyabikere	Waga	Rutovu
SiO_2	49.88	49.08	49.70	51.03	52.44	53.01	52.88	47.81	55.20	61.32	48.53	48.59	47.72	48.18	47.91	50.69
TiO_2	0.61	0.41	027	0.58	0.44	0.57	0.65	0.76	0.49	1.63	1.72	1.63	1.71	1.61	1.20	1.44
Al_2O_3	14.63	15.53	1560	14.59	15.95	13.75	1455	15.62	14.84	13.83	14.14	14.15	12.93	14.00	13.49	13.77
Fe_2O_3	14.15	13.86	11.71	14.78	9.50	10.49	10.35	12.21	10.34	12.46	13.96	13.09	14.21	14.09	14.10	13.02
MnO	0.20	0.22	0.19	0.20	0.14	0.16	0.21	0.20	0.15	0.18	0.23	0.20	0.23	0.26	0.23	0.19
MgO	7.89	8.18	7.87	7.00	7.16	8.85	7.49	10.42	6.30	1.92	6.80	7.43	7.48	6.57	7.96	7.12
CaO	12.54	11.93	13.50	10.43	11.05	9.40	9.30	11.05	9.20	5.80	11.83	12.28	12.06	12.43	12.42	11.72
Na_2O	1.54	1.33	1.35	2.02	1.33	0.90	1.13	1.07	1.95	1.78	2.59	2.38	2.34	1.57	1.82	1.53
K_2O	0.13	0.08	0.16	0.19	0.22	0.27	0.46	0.16	1.29	1.20	0.34	0.32	0.29	0.31	0.13	0.19
P_2O_5	0.01	0.02	0.01	0.02	0.21	0.14	0.27	0.07	0.15	0.36	0.20	0.18	0.18	0.13	0.10	0.12
Total	101.58	100.64	100.36	100.84	98.44	97.54	97.29	99.37	99.91	100.48	100.34	100.25	99.15	99.15	99.36	99.79
U	0.08	0.15	0.12	0.13	0.7	1.2	1.3		1.1	3.1	0.8	0.5	0.4	0.4	0.2	0.2
Th	0.06	0.43	0.25	0.39	1.5	3.6	3.7	0.9	4.3	11.8	1.7	1.0	1.5	1.4		0.4
Zr	8	11	12	32	66	78	82	79	106	232	105	103	113	106	65	73
Hf	0.32	0.42	0.55	1.0	2.3	2.6	2.9	2.0	3.5	6.6	2.9	3.2	3.0	3.1	1.6	2.3
Nb	0.08	1.5	0.7	3.2	2.8	3.7	4.1	6.7	3.0	25	17	17	21	19	< 4	4.7
Ta	0.02	0.06	0.14	0.24	0.35	0.44	0.47	0.40	0.50	1.73	1.00	< 1	1.32	1.26	< 1	0.34
Rb	3.7	1.7	4.7	4.0	14	25	23	8	51	72	12	11	11	9	2.5	2.1
Sr	137	130	163	139	118	98	126	117	216	160	203	222	223	216	126	128
Ba	35	55	61	101	130	90	150	99	331	277	144	128	128	135	30	66
Ni	27	9	12	31				12	60	12	68	113	93	113	100	57
V	413	259	128	220	221	245	230	272	149	55	299	267	287	254	311	286
Cr	386	206	247	184	265	604	384	630	51	47	120	290	205	219	180	83
Zn	77	82	77	103	55	68	53	75	84	120	79	72	108	117	82	71
Co	44	36	26	41	29	39	36	46	12	10	55	55	51	47	57	35
Cu	17	18	18	503						19			95	152		35
Ga	16	12	10	17						23			19	19		16
Y	7.7	9.5	15.0	15.0	19.0	22.9	23.5	22.0	30.0	57.4	34.0	31.0	27.9	26.2	30.0	24.2
La	1.82	3.84	3.80	7.71	11.50	13.00	13.80	11.40	20.57	59.14	14.50	15.00	12.49	12.07	4.10	4.64
Ce	2.94	6.30	7.59	15.66	23.80	27.90	29.60	25.86	43.11	88.87	31.00	33.00	28.39	27.55	11.00	11.87
Pr	0.47	0.84	1.23	1.88	3.40	4.00	4.20	3.32	5.51	14.07			3.77	3.70		1.99
Nd	2.28	3.78	5.80	8.82	12.80	14.40	14.90	13.72	22.47	59.82	16.00	17.00	17.17	16.63	8.00	9.73
Sm	0.78	1.06	1.84	2.28	2.60	3.10	3.30	3.14	4.50	13.25	3.60	3.70	4.69	4.31	2.40	3.13
Eu	0.62	0.87	0.79	0.96	0.74	0.95	0.96	0.91	1.17	3.49	1.90	1.50	1.73	1.64	0.90	1.20
Gd	107	1.34	2.36	2.39	2.50	3.40	3.40	3.47	4.63	12.52			5.11	4.80		3.86
Tb	0.20	0.25	0.41	0.40	0.40	0.64	0.71	0.50		1.88	0.80	0.70	0.83	0.82	0.80	0.65
Dy	1.29	1.54	2.69	2.73	2.70	3.20	3.50	3.66	4.71	10.59			4.97	4.78		4.31
Ho	0.30	0.35	0.60	0.61	0.68	0.82	0.82	0.73	0.90	2.03			1.06	0.98		0.89
Er	0.86	1.08	1.76	1.76	1.90	2.10	2.32	2.15	2.86	5.64			2.94	2.73		2.64
Tm	0.12	0.18	0.26	0.29	0.29		0.34			0.78			0.45	0.39		0.42

Yb	0.90	1.13	1.85	1.81	1.84	1.98	2.21	2.17	2.96	4.99	2.70	2.60	2.81	2.71	2.10	2.69
Lu	0.14	0.17	0.26	0.27	0.34	0.33	0.36	0.32	0.45	0.71	0.39	0.39	0.40	0.40	0.31	0.37
Eu/Eu*	2.08	2.23	1.16	1.25	0.88	0.89	0.87	0.84	0.78	0.82	1.43	1.15	1.08	1.10	0.88	1.06
mg#	53	54	57	49	60	63	59	63	55	24	49	53	51	48	53	52

Major element by XRF on calcinated samples and trace elements by ICP–MS (CIGI, ULG).

Sample location and type: SG23C: Nyanga-Songa intrusion, road Nyange-Mosso, boulders of microgranular gabbro; BU92: Buhoro intrusion, Gihamagara valley, boulders of microgranular gabbronorite; BU78: Buhoro intrusion, E of Gihamba valleys, boulders of mesocratic fine-grained massive gabbronorite; RU10: Rutovu intrusion, Gasenyi valley, boulders of microgranular gabbronorites (with pyroxene oikocrysts); BU93: Buhoro massif, valley S of Gihamaraga, microgabbronorite boulders; 93BU4 and 93BU5: S Mukanda-Buhoro massif, 2 km SE of Mwishanga dolerite dikes crosscuting the Nyamabuye sub-formation; BU17: Buhoro massif, Mpame, bridge over river Nyakijanda, subophitic microgabbro boulders; A117B: Rutovu massif, bridge over Gasenyi river, amphibole bearing dolerite; NY P176: Nyabikere intrusion, NE Rwandagaro, granophyre; NY P142: Nyabikere intrusion, Ntaruka river, subophitic microgabbro boulders; NY P145: Nyabikere intrusion, Ntaruka river, subophitic microgabbro boulder; NY P138: Nyabikere intrusion, Ntaruka river, dolerite boulder; NY80: Nyabikere intrusion, N of Nyarunazi, affluent to Ntaruka stream. Olivine bearing subophitic microgabbro; W26: Waga intrusion, 1 km Wof Kabundugu, subophitic microgabbro fragments in laterite; RU04: Rutovu massif, sources of the Nile, dolerile dyke.

(Tack et al., 1994). Sr and Nd data, calculated for an age of 1275 Ma, are plotted in Fig. 11. In the case of a 1370 Ma age for the emplacement of the KM intrusions, ε_{Nd} values would be modified by less than $|\varepsilon|$, whereas Sr initial ratios would not be significantly modified because of low Rb contents. These variations would thus not affect our conclusions. Two groups of samples distinctly appear: the first one, with negative $\varepsilon_{Nd(1275\,Ma)}$ values and high Sr initial compositions, includes the Mukanda-Buhoro melts, defined above, and cumulates from the Mukanda-Buhoro and Musongati bodies. The second group, with depleted mantle values, comprises the Nyabikere and the Waga fine-grained rocks (the Rutovu dolerite with high Sr isotope ratio and positive ε_{Nd} has been perturbed and should be ignored).

Interestingly, the cumulate samples from Nyabikere (Table 3) show high Sr initial ratios, similar to those in the other layered intrusions. It can be concluded that the Mukanda-Buhoro melts and cumulates are comagmatic, and, on the other hand, that the Nyabikere melts are not related to the cumulates of this intrusion. As for the Waga intrusions, isotopic data on the cumulate rocks are lacking, thus precluding a comparison with the doleritic rock.

These data corroborate previous conclusions regarding the existence of two distinct differentiation trends and sources for the Kabanga-Musongati layered intrusions and for the A-type granitoids of Burundi, respectively (Tack et al., 1994). We confirm that, paradoxically, the Kabanga–Musongati source is an enriched one, possibly the subcontinental lithospheric mantle, and that the A-type granitoid source is a depleted asthenospheric mantle. The depleted source of the Nyabikere and Waga dolerites indicates that they are not linked to the Kabanga–Musongati mafic–ultramafic magmatism. Their source characteristics could suggest that they are related to the A-type granitoid magmatism, but this link has to be further investigated.

6.3. Modelling the melt–cumulate relationships

Sample BU17 from the Mukanda-Buhoro group has already been considered as a possible "chilled" magma (Tack et al., 1994). Since this sample, with 10.4% MgO, is the most primitive composition of the Mukanda-Buhoro group that we have identified, it is worthwhile determining the nature and composition of its liquidus minerals. Modelling of this composition using MIXNFRAC algorithm (Nielsen, 1989) and assuming a 3 kbar pressure and oxygen fugacity at the FMQ buffer, is reported in Table 4. It can be seen that the first mineral to appear at the liquidus is Fo_{88}, a value matching the olivine composition in lherzolite (see Fig. 4). This liquid can thus produce a lherzolite cumulate similar to those of Musongati. It should be noted, however, that

Table 3
Sr and Nd isotope data from fine-grained rocks and cumulates from Kabanga–Musongati intrusions

	Rb (ppm)	Sr (ppm)	$^{87}Rb/^{86}Sr$	$^{87}Sr/^{86}Sr \pm 2\sigma_m(*10^{-6})$	ISr(1275 Ma)	Sm (ppm)	Nd (ppm)	$^{147}Sm/^{144}Nd$	$^{143}Nd/^{144}Nd \pm 2\sigma_m(*10^{-6})$	$\varepsilon_{Nd(1275\,Ma)}$	T_{CHUR}	T_{DM}
Fine-grained rocks												
Mukanda-Buhoro group												
BU17*	8.3	116.6	0.2061	0.712980 ± 30	0.709215	15.70	64.10	0.14812	0.511987 ± 9	−4.78	2307	2468
BU93	14.4	118.0	0.3535	0.718671 ± 10	0.712212	2.60	12.80	0.12283	0.511776 ± 14	−4.76	2043	2126
93 BU5	23.3	126.0	0.5359	0.721624 ± 9	0.711834	3.30	14.90	0.13393	0.511868 ± 13	−4.78	2141	2249
93 BU4	25.1	98.2	0.7408	0.723933 ± 9	0.710398	3.10	14.40	0.13018	0.511886 ± 15	−3.82	2025	2112
Nyabikere group												
NY 80	9.5	215.6	0.1273	0.704109 ± 10	0.701783	4.31	16.63	0.15685	0.512565 ± 10	5.10	1274	–
NYP142	12.0	203.0	0.1710	0.704594 ± 10	0.701470	3.60	16.00	0.13608	0.512545 ± 10	8.11	1002	982
NYP145	11.0	222.0	0.1433	0.704435 ± 8	0.701816	3.70	17.00	0.13164	0.512541 ± 9	8.76	960	938
Waga and Rutovu group												
W 26	2.5	126.0	0.0574	0.703076 ± 8	0.702027	2.40	8.00	0.18146	0.512837 ± 9	6.39	1026	–
RU 04	2.1	127.6	0.0484	0.713017 ± 11	0.712132	3.13	9.73	0.19491	0.512835 ± 11	4.15	1544	–
Cumulates												
BU30*	1.2	157.2	0.0221	0.708900 ± 50	0.708496	0.73	2.24	0.19709	0.512233 ± 29	−7.99	5291	–
BU78*	4.7	162.9	0.0835	0.7118S0 ± 30	0.710354	2.38	8.00	0.17992	0.512193 ± 20	−5.96	3296	–
MU39*	5.4	112.8	0.1386	0.713580 ± 30	0.711048	0.67	3.13	0,12944	0.511759 ± 10	−6.18	2216	2329
NYP128	2.10	47.3	0.1253	0.711080 ± 50	0.708788							
NYP141	6.70	134	0.1447	0.711060 ± 40	0.708416							
NY33	5.90	71.2	0.2386	0.712122 ± 13	0.707762							
NY65	11.40	205	0.1611	0.713363 ± 9	0.710419							
NYP141-Plag	6.60	255	0.0747	0.709964 ± 8	0.708600							

Sample location and rock type: BU30: Buhoro intrusion. SW of Nyarurambi, layered gabbronorite cumulate; BU78: Buhoro intrusion, SSW of Gihamba, fine-grained gabbronorite; MU39; Musongati intrusion, Nyamabuye stream near Muhoza, noritic cumulate boulders; NYP128: Nyabikere intrusion. Ntaruka river NNE of Nyarunazi, pyroxenite (boulders); NYP141: Nyabikere intrusion, norite cumulate (boulders): NYP141: Plag; Nyabikere intrusion, plagioclase separated from the previous samples; NY33: Nyabikere intrusion, S of Rwakagari, fine-grained gabbronorite (boulders); NY65: Nyabikere intrusion. Ntaruka river S of Mubanga, gabbronorite (boulders); Rock type and location of all other samples: see Table 2. T_{DM} model ages are given for samples having $^{147}Sm/^{144}Nd < 0.15$.

Samples marked by an *are from Tack et al. (1994).

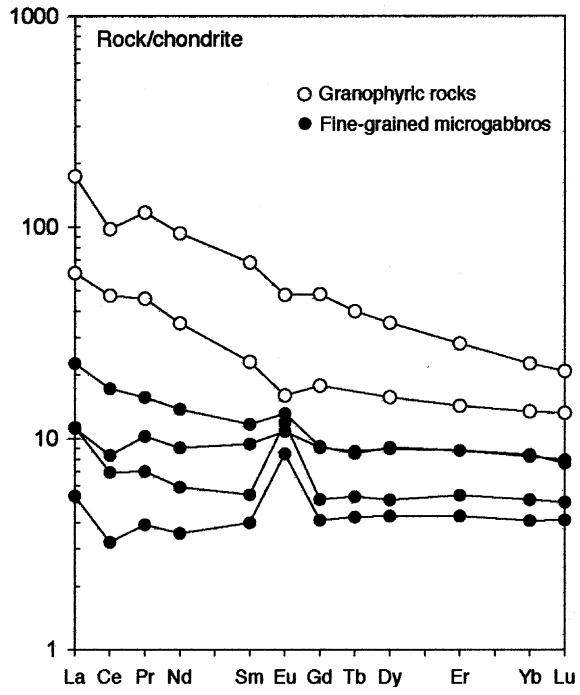

Fig. 9. Chondrite-normalized REE composition in granophyric rocks (filled square) and in fine-grained microgabbros (open circle).

olivine crystallised alone only over a short interval (4%), which precludes the formation of large quantities of ultramafic cumulates. Moreover, the composition of the olivine in dunite is slightly more Mg rich (Fo_{90}), which calls for a melt richer in MgO than BU17. It can thus be concluded that BU17 is not parental to the Musongati body, but is already more evolved. This in turn suggests that the parental magma tends towards a picritic composition.

Other compositions (BU93 and NYP) have also been modelled and the results are reported in Table 4. Plagioclase is the first liquidus mineral in both cases and therefore these melts are not suitable as parent liquids for the ultramafic intrusions nor for the gabbronorite intrusions (the calculated plagioclase An_{78} for NYP is too anorthite-rich).

It should be further noted that the three melts which have been modelled produce troctolite over large intervals of crystallization, and not pyroxenite and norite. This feature is actually an artefact of Nielsen's algorithm: the model artificially delays the appearance of liquidus orthopyroxene, as observed in the Bushveld Complex (Cawthorn, pers. comm.) and in several other cases (Duchesne, unpubl.).

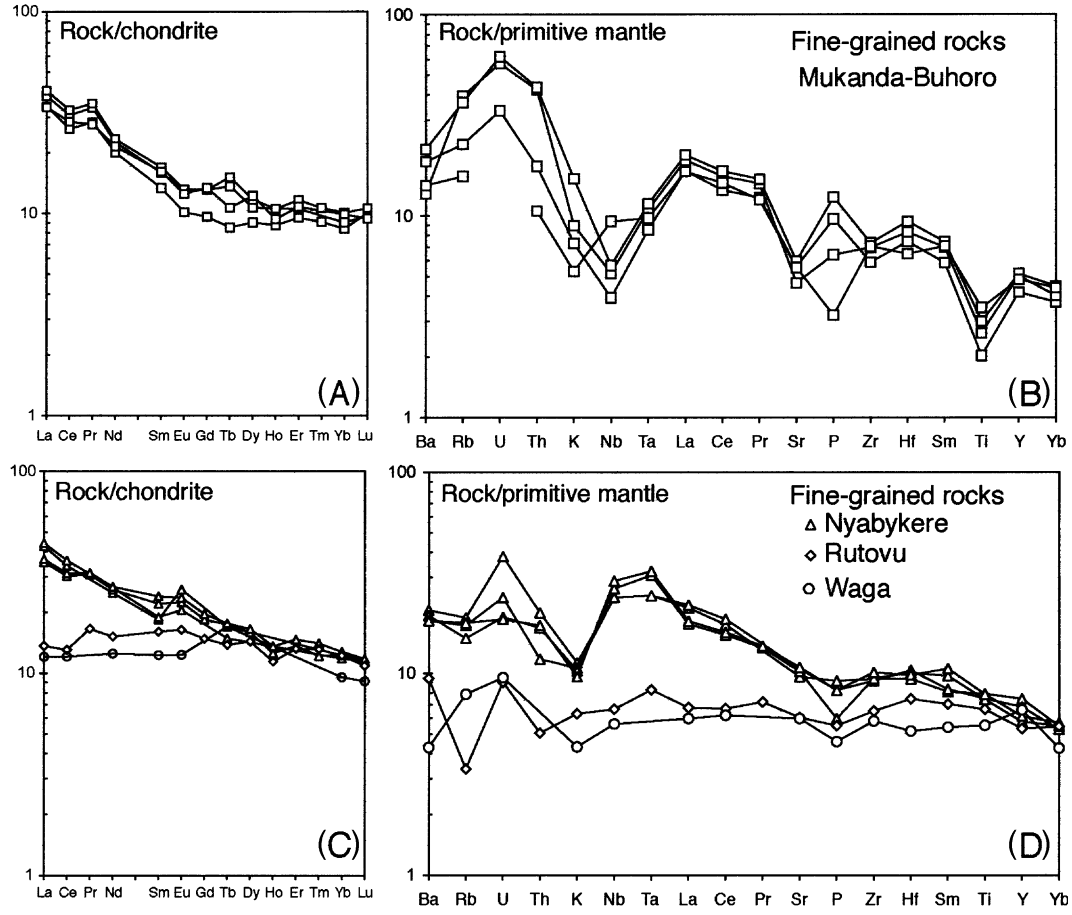

Fig. 10. Chondrite-normalized trace element composition of fine-grained rocks: (A, B) Mukanda-Buhoro fine-grained rocks; (C,D) Nyabikere, Rutovu and Waga fine-grained rocks. Spidergram normalizing values from Thompson et al. (1984).

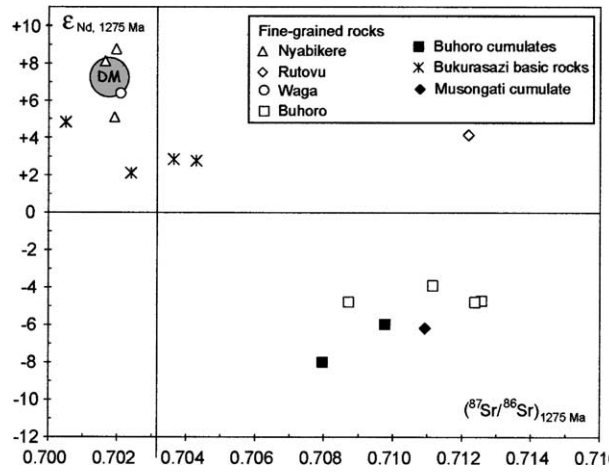

Fig. 11. $\varepsilon_{Nd(1275\,Ma)}$ vs. Sr initial ratio (1275 Ma) in Mukanda-Buhoro, Nyabikere, Waga and Rutovu fine-grained rocks and in Mukanda-Buhoro and Musongati cumulate rocks. Values from Bukirasazi mafic rocks (Tack et al., 1994) are also given for comparison.

Table 4
MIXNFRAC modelling of fractional crystallization (3 kbar and fO_2 at FMQ) of possible parental magmas

BU17 (Mukanda-Buhoro type, Mg-rich)
0% 1257 °C Fo_{88} (peridotite)
4% 1228 °C Fo_{85} + An_{86} (troctolite)
46% 1162 °C Fo_{75} + An_{83} + Aug (olivine gabbro)
BU93 (Mukanda-Buhoro type, Mg-poor)
0% 1233 °C An_{84} (anorthosite)
6% 1200 °C An_{82} + Fo_{85} (troctolite)
28% 1167 °C An_{80} + Fo_{81} + Aug (olivine gabbro)
NYP (average of 4 samples) (Nyabikere type)
0% 1204 °C An_{78} (anorthosite)
5% 1188 °C An_{77} + Fo_{80} (troctolite)
20%1160 °C An_{74} + Fo_{76} + Aug (olivine gabbro)

7. The two magma hypothesis

Though it is difficult to assess the composition of the parental magmas, due to the lack of chilled margin and adequate dyke rocks, some general features point to the possibility of two distinct magma compositions having been involved in the evolution of the KM mafic and ultramafic intrusions.

The marked difference of bulk compositions of the intrusions is notable and not due to a possible variation of the level of erosion. The intrusions dip ≈60° to the west so that both the floor and roof of the magma chambers can be observed in some places despite locally developed thrust faulting in the contact zones. As already pointed out, some bodies (e.g. Mugina, Nyange-Songa, Rutovu, Mukanda-Buhoro) comprise only anorthosite and gabbronorite, with the latter lithology lying directly on the floor (Fig. 2). The Waga body consist exclusively of ultramafic rocks. In Muremera, Nyabikere and Musongati, ultramafic rocks dominate over plagioclase-bearing rocks, and, in the latter body, dunite, lherzolite and pyroxenite-peridotite represent more than 66% of the area (Deblond, 1994).

The parental magma of the Musongati body was likely to have been picritic, as also suggested for the Kabanga intrusion (Evans et al., 2000), thus reducing the availability of evolved residual liquids necessary to form gabbronoritic and anorthositic cumulates. Nowhere has a transition from norite to gabbronorite been observed in the mafic intrusions. Indeed, the gabbronorites of the Mukanda-Buhoro body are clearly separated by a septum (Fig. 2) of metasediments from the most evolved norites of the Musongati body. In other words, it appears that the geographical contiguity between the Mukanda-Buhoro and the Musongati bodies is coincidental rather than petrogenetically significant. A relatively large gap in mineral composition is observed (Fig. 4) between the Musongati norites (An_{89-86} and opx mg# 79–75 in norite) and the Mukanda-Buhoro gabbronorites (An_{75-58} and opx mg# 58–45).

None of the previous characteristics provide decisive evidence for the existence of two parental magmas. But if this hypothesis is accepted, the analogies with the Bushveld Complex, already mentioned for the petrographical similarities between gabbronorites from both occurrences, become even stronger. Indeed, several magma influxes have been invoked to account for the huge volume of the Bushveld Complex (see discussion in Cawthorn, 1996). Particularly two influxes seem to be important there: the Lower and Critical Zone magma, probably of picritic composition, and the Main Zone magma, more evolved in composition, and of huge lateral extension. We incline to the view that similar magmas can be invoked in the KM alignment in Burundi. The first magma would be a picritic basalt, but, contrary to the Bushveld Complex, it was unable to produce chromitite (e.g. Musongati, Waga). The second one, giving rise to gabbronorite and anorthosite, would be analogous to the Main Zone magma (e.g. Mugina, Nyange-Songa, Rutovu, Mukanda-Buhoro) and also shows a large geographical extension. In contrast to the Bushveld case, there is, however, not much difference in isotopic signature between the two magmas. Apparently, they came from isotopically similar sources. Alternatively it is not precluded that the second magma, parental to the mafic intrusions, might be derived from the picritic magma by fractional crystallisation in a deeper level magma chamber. If this is the case, the absence of gabbronoritic rocks and anorthosites in the ultramafic intrusions nevertheless remains intriguing.

8. Conclusions

The Kabanga–Musongati layered intrusions are distributed into ultramafic and gabbronoritic types of bod-

ies, which both form an alignment in a weakness zone between the Kibaran belt and the Tanzania craton (Tack et al., 1994, 2002). The intrusions display, when considered as a whole, a classical series of cumulates from dunite to anorthosite with well-defined cryptic layering (Deblond, 1994). Fractional crystallization was the dominant differentiation mechanism. The Cr–Ni behaviour in the melt precludes the occurrence of large chromitite and Ni sulphide concentrations associated with the ultramafic rocks.

Several lines of evidence point to the occurrence of two types of magma to form the various bodies. The first one, a picritic basalt, has given rise to the ultramafic bodies. The second one, analogous to the Main Zone magma of the Bushveld Complex, has formed the gabbronorite bodies. Both magmas came from the same enriched mantle source, characterized by negative ε_{Nd} values and high Sr isotope initial ratios, indicative of an old subcontinental lithospheric mantle.

In the same weakness zone, A-type granitoids and doleritic dykes have also been emplaced but they possess a clearly distinct depleted asthenospheric mantle signature.

Acknowledgments

Major and trace element analyses were performed at the CIGI (University of Liège) by G. Bologne. The Belgian "Direction Générale pour la Coopération au Développement" (DGCD) is thanked for supporting the Doctorat thesis of A. Deblond (BDI/CI 14497/11) and a University Cooperation Programme with the University of Burundi at Bujumbura. The paper has benefited from constructive reviews of J. R. Wilson and D. M. Evans, who are sincerely thanked.

References

Cawthorn, R.G., 1996. Layered Igneous Rocks. Elsevier, Amsterdam, 531p.

Deblond, A., 1993. Géologie et pétrologie des massifs basiques de la ceinture Kabanga-Musongati au Burundi. Doctorat dissertation. University of Liège, Belgium, 235p.

Deblond, A., 1994. Géologie et pétrologie des massifs basiques et ultrabasiques de la ceinture Kabanga-Musongati au Burundi. Annales du Musée Royal de l'Afrique Centrale Tervuren Sciences géologiques 99, 1–123.

Deblond, A., Tack, L., 1999. Main characteristics and review of mineral resources of the Kabanga–Musongati alignment in Burundi. Journal of African Earth Sciences 29, 313–328.

Evans, A.M., 1993. Ore Geology and Industrial Minerals. An Introduction. Blackwell Science, Oxford, 389p.

Evans, D.M., Byemelwa, L., Gilligan, J., 1999. Variability of magmatic sulphide compositions at the Kabanga nickel prospect, Tanzania. Journal of African Earth Sciences 29, 329–351.

Evans, D.M., Boadi, I., Byemelwa, J., Gilligan, J., Kabete, J., Marcet, P., 2000. Kabanga magmatic nickel suphide deposits, Tanzania: morphology and geochemistry of associated intrusions. Journal of African Earth Sciences 30, 651–674.

Kruger, F.J., 1994. The Sr-isotopic stratigraphy of the western Bushveld Complex. South African Journal of Geology 97, 393–398.

Lee, C.A., 1996. A review of mineralization in the Bushveld Complex and some other layered mafic intrusions. In: Cawthorn, R.G. (Ed.), Layered Intrusions. Elsevier, Amsterdam.

Naldrett, A.J., 1989. Magmatic Sulfide Deposits. Oxford University Press, Oxford, 186p.

Naldrett, A.J., Cameron, G., von Grunewaldt, G., Sharpe, M.R., 1987. The formation of stratiform PGE deposits in layered intrusions. In: Parsons, I. (Ed.), Origin of Igneous Layering, NATO ASI Series. Reidel, Dordrecht, pp. 313–398.

Nielsen, R.L., 1989. Phase equilibria constraints on liquid lines of descent generated by paired assimilation and fractional crystallization: trace elements and Sr and Nd isotopes. Journal of Geophysical Research 94, 787–794.

Rollinson, H., 1993. Using Geochemical Data: Evaluation, Presentation, Interpretation. Longman Scientific and Technical, Harlow, 352p.

Simkin, T., Smith, J.V., 1970. Minor element distribution in olivine. Journal of Geology 78, 304–325.

Tack, L., Deblond, A., 1990. Intrusive character of the Late Kibaran magmatism in Burundi. IGCP No. 255 Newsletter 3, 81–87.

Tack, L., Liegeois, J.-P., Deblond, A., Duchesne, J.C., 1994. Kibaran A-type granitoids and mafic rocks generated by two mantle sources in a late orogenic setting (Burundi). Precambrian Research 68, 323–356.

Tack, L., Fernandez-Alonso, M., Tahon, A., Wingate, M., Barritt, S., 2002. The "Northeastern Kibaran Belt" (NKB) and its mineralisations reconsidered: new constraints from a revised lithostratigraphy, a GIS-compilation of existing geological maps and a review of recently published as well as unpublished igneous emplacement ages in Burundi. 11th Quadrennial IAGOD Symposium and GEOCONGRESS 2002, 22–26 July 2002, Windhoek, Namibia, Extended Abstract on CD-Rom and Synopsis in Conference Programme, p. 42.

Thompson, J.F.H., Naldrett, A.J., 1984. Sulfide–silicate reactions as a guide to Ni–Cu–Co mineralization in central Maine. In: Buchanan, D.L., Jones, M.J. (Eds.), Sulfide Deposits in Mafic and Ultramafic Rocks. Institute of Mining and Metallurgy Special Publication, London, pp. 103–113.

Thompson, R.N., Morrison, M.A., Hendry, G.L., Parry, S.J., 1984. An assessment of the relative roles of crust and mantle in magma genesis: an elemental approach. Philosophical Transactions of the Royal Society of London A310, 549–590.

von Grünewaldt, G., 1990. On the phase change orthopyroxene pigeonite and the resulting textures in the Main and Upper zones of the Bushveld Complex in Eastern Transvaal. Geological Society of South Africa Special publication 1, 67–73.

Wager, L.R., Brown, G.M., 1968. Layered igneous rocks. Oliver and Boyd Ltd, London, 588p.